

Received January 31, 2020, accepted March 19, 2020, date of publication March 26, 2020, date of current version April 22, 2020.

Digital Object Identifier 10.1109/ACCESS.2020.2983492

# Design of WPT RF Power Supply Based on Dual Directional Coupler and Capacitor Array Impedance Matching Network

ZHIHUI HUANG<sup>1</sup>, (Member, IEEE), LEI WANG<sup>1</sup>, (Student Member, IEEE),  
YUXING ZHANG<sup>1</sup>, (Student Member, IEEE), AND RUITONG LIU<sup>2</sup>

<sup>1</sup>School of Electrical Engineering, Dalian University of Technology, Dalian 116024, China

<sup>2</sup>Electric Power Research Institute of State Grid Liaoning Electric Power Company, Ltd., Shenyang 110006, China

Corresponding author: Zhihui Huang (huangzhihui@dlut.edu.cn)

This work was supported by the Science and Technology Project of State Grid in 2017 under Grant CB17-2017GW-21.

**ABSTRACT** In the engineering use of a magnetically coupled resonant radio energy transmission system, both the resonant frequency and the optimal load impedance will be varied because of the external conditions. In view of the above problems, this paper proposes an RF power supply with adjustable frequency and optimal load impedance, in order to achieve efficient power transmission for different frequency radio energy transmission systems and different load conditions. The RF power supply is mainly composed of a frequency controllable signal generator, a Class E power amplifier circuit, a dynamic impedance matching network, a load detection circuit and a controller. Through the above parts, the load tracking of the RF power supply can be realized, and the higher output efficiency can be realized under the condition of changing the working frequency and the load. Finally, the feasibility of the proposed RF power supply is verified through experiments. The experimental results show that the RF power supply can automatically track changes in the operating frequency and load range, and the output efficiency can be maintained at more than 75%.

**INDEX TERMS** Load tracking, magnetic coupling resonance, RF power supply, wireless power transmission.

## I. INTRODUCTION

The magnetically coupled resonant radio energy transmission technology was first proposed by Professor Marin Siljacic of the Massachusetts Institute of Technology (MIT) at the AIP Industrial Physics Forum in the United States in November 2006. In 2007, their team successfully used a magnetically coupled resonant radio energy transmission technology to achieve a 60-watt bulb illuminated at a distance of 2m [1]–[3]. As a medium-range radio energy transmission technology, this technology can achieve high-efficiency, high-power radio transmission at medium distances compared to other types of radio energy transmission technology. It provides a new solution for many occasions where it is inconvenient to transmit power through wires, and has a good development prospect [4], [5].

At present, the research on magnetically coupled resonant wireless energy transmission systems under constant fre-

quency and constant load conditions is relatively mature, and higher efficiency energy transmission can be achieved under the condition that the working conditions are fixed. However, in actual engineering use, the load of a wireless power transmission system is changed in most cases, and its resonance frequency is also affected by various factors. Reference [6] proposed the use of wireless energy transmission systems for lithium battery charging. At different stages of battery charging, as the load of the wireless power transmission system, the equivalent impedance of the lithium battery is a changing value. How to ensure that the wireless power transmission system maintains high efficiency during the entire charging process is still worthy of our study. In addition, research is being conducted on the power supply of high-voltage equipment on outdoor high-voltage transmission lines using wireless power transmission systems. Some studies have pointed out that the resonance frequency of the coupling coil in a wireless power transmission system may vary by  $\pm 10\%$  due to the influence of external conditions. This article mainly focuses on how to improve the power conversion efficiency

The associate editor coordinating the review of this manuscript and approving it for publication was Vittorio Camarchia<sup>1</sup>.

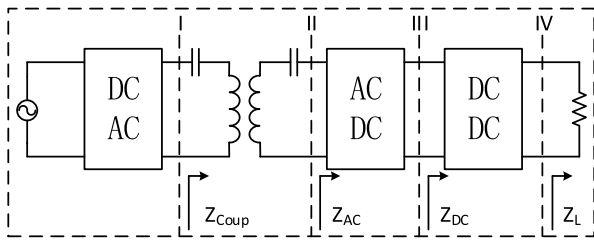


FIGURE 1. Implementation scheme of wireless energy transmission system.

of RF power in wireless power transmission systems under variable frequency and variable load conditions. The current implementation scheme of the wireless energy transmission system is shown in Figure 1. It mainly includes the power supply terminal, the coupling coil, and the load terminal. At present, researches on how to ensure the transmission efficiency of a wireless power transmission system under a variable load situation are mainly focused on the load side. They change the load impedance to the optimal impedance of the wireless power transmission system through the AC/DC or DC/DC conversion circuits at the output. In this way,  $Z_{AC}$  or  $Z_{DC}$  in Figure 1 is a fixed impedance. Reference [7] proposed adding step-down chopper circuit and energy storage equipment failure efficiency control and power control at the load end. Reference [8] proposes to directly calculate the load impedance by directly measuring the voltage and current across the load connected to the wireless power transmission system, and realize the impedance change at the output through the buck circuit to improve system efficiency. These solutions for designing impedance change circuits at the load end are often designed for specific loads, and their versatility is poor. In addition, there is another implementation scheme. That is to add a wireless communication system at the transmitting end and the receiving end respectively to achieve closed-loop control and improve system efficiency [9], [10], but this solution increases the transmission of wireless data in wireless energy systems. The circuit increases the complexity of the system. Whether the wireless power transmission system will affect the communication system under the condition of large transmission power requires further research.

In view of the above problems, this paper proposes a design scheme of an RF power supply with adjustable frequency and optimal load. The dynamic impedance matching at the power supply side can better shield the difference of the load and avoid the introduction of a more loaded communication scheme. Optimize the transmission efficiency with a simpler system structure design.

## II. SYSTEM COMPOSITION

The main structure of the RF power supply is shown in Figure 2. It mainly includes five parts: frequency controllable signal source, class E power amplifier circuit, dynamic impedance matching network, load impedance detection circuit and control system. The frequency controllable signal source can be controlled by the controller to achieve dynamic

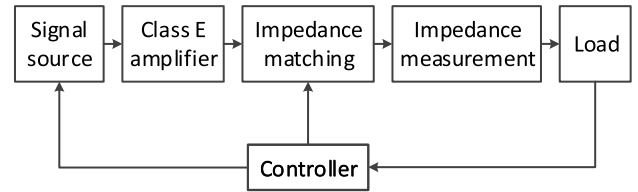


FIGURE 2. The overall implementation of RF power supply.

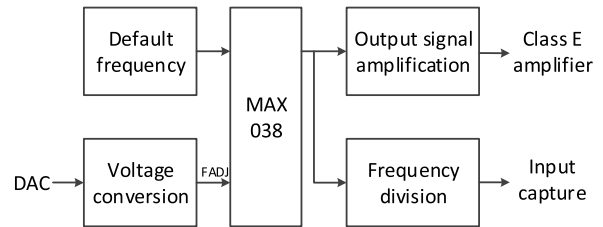


FIGURE 3. Design scheme of frequency controllable signal generator.

frequency adjustment and amplify the output signal power to the input power required by the class E power amplifier. The class E power amplifier circuit realizes power amplification of the signal source output signal. The load impedance detection circuit realizes the identification of the load connected to the latter stage and provides a feedback signal for the dynamic impedance matching network. The dynamic impedance matching network realizes real-time impedance matching of the output impedance of the class E power amplifier circuit to the load impedance according to the feedback signal of the load impedance detecting circuit. Finally, through the control system to achieve the overall cooperation of the above four parts, the RF power supply can achieve efficient power output for different frequencies and different load impedances.

### A. FREQUENCY CONTROLLABLE SIGNAL SOURCE

The signal source mainly provides the input signal for the RF power supply and amplifies it to the value required by the power amplifier for the input signal. This paper intends to use the high frequency precision function signal generator MAX038 as the signal source. This analog IC can achieve a sine wave output of 0.1-20MHz, and its output frequency can be dynamically adjusted by setting the FADJ pin voltage to 0.3~1.7 times the fundamental frequency. It is well suited to the design requirements of this article. The main structure of the signal source is shown in Figure 3:

In Figure 3, MAX038 is the signal generator. After setting the MAX038 fundamental frequency at the center frequency of the system operation, the controller's digital-to-analog converter (DAC) output is level-converted and connected to the MAX038's FADJ pin. We can control the output frequency of MAX038 by controlling the voltage of FADJ pin. The output signal of MAX038 is connected to a signal amplifying circuit and a frequency dividing circuit respectively. The peak-to-peak value of the output signal of MAX038 is 2V. The signal amplification circuit amplifies the output signal of MAX038 to 22~23dbm for driving the class E power

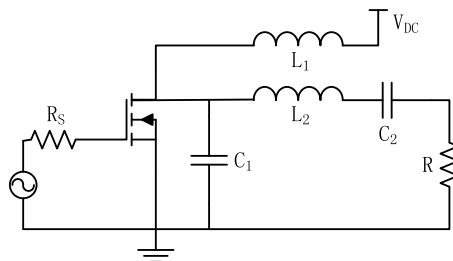


FIGURE 4. Class E power amplifier structure.

amplifier (the output impedance of the signal source and the input impedance of the class E power amplifier are matched to  $50\Omega$ ). The frequency dividing circuit divides the output signal by 256 and then connects to the controlled input capture channel. The MAX038 output frequency measurement is achieved by measuring the period of the divided signal to provide a feedback signal for the precise output of the frequency.

### B. CLASS E POWER AMPLIFIER CIRCUIT

Class E power amplifier can be regarded as a DC-AC inverter. This type of amplifier is mainly divided into Zero Voltage Switching (ZVS) type and Zero Current Switching (ZCS) type. Among them, ZVS type E power amplifier is considered to be the most efficient amplifier [11]. The classic zero-E power amplifier structure is shown in Figure 4:

In Figure 4,  $L_1$  is a choke inductor and  $C_1$  is a transistor bypass capacitor.  $L_2$  and  $C_2$  together form a filter network for class E power amplifiers. When the class E power amplifier operates in the ZVS state, the choke inductor  $L_1$  and the LCR series resonant circuit can be equivalent to one current source. When the transistor is turned on, current flows through the switching transistor. When the transistor is turned off, current flows through the bypass capacitor and generates a voltage across the bypass capacitor and the transistor. Therefore, the bypass capacitor determines the voltage waveform across the transistor.

### C. DYNAMIC IMPEDANCE MATCHING NETWORK

Commonly used circuits in impedance matching networks include L-type,  $\pi$ -type, T-type, etc [12]. In the case of low frequency (the wavelength of the electromagnetic wave is much larger than the board size), the above circuit is usually built by using an inductor and a capacitor. In actual engineering use, the magnitude of the inductance can be changed by changing the position of the core. However, the inductance used in this subject has a small inductance value, and the Q value of the inductor with a magnetic core is difficult to be high. In practice, the hollow inductor is generally used to complete the impedance matching. Therefore, changing the inductance value is difficult to achieve.

The capacitance value can be changed by changing the relative area of the parallel plate capacitors, or by changing the capacitance values by connecting different sizes of capacitors. Changing the relative area of parallel plate capacitors requires designing complex mechanical structures, and the

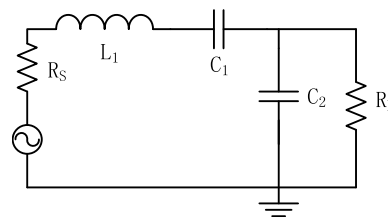


FIGURE 5. impedance matching network.

difference in the mechanical structure's dead space affects the accuracy of capacitance adjustment. And the external environment also has a certain influence on the capacitance value, so it is difficult to obtain accurate control of the capacitance value. According to the above situation, this paper uses the latter scheme to achieve the change of capacitance value. For the selection of the actual circuit of the impedance matching network, this paper implements dynamic impedance matching through a deformed L-type impedance matching network. As shown in Figure 5:

In Figure 5,  $L_1$  is a series inductor,  $C_1$  is a series capacitor, and  $C_2$  is a shunt capacitor. Where  $L_1$  is designed to be a fixed value, and  $C_1$  and  $L_1$  are connected in series to form a reactance value in the series circuit. By changing the size of  $C_1$ , the series reactance value can be dynamically changed. Changing  $C_2$  can change the reactance value of the parallel connection, thereby achieving dynamic impedance matching.

### D. LOAD IMPEDANCE DETECTION CIRCUIT AND CONTROL SYSTEM

The load impedance detection circuit mainly detects the size of the overall impedance connected to the RF power supply ( $Z_{\text{coup}}$  in Figure 1). The value of the impedance is passed into the control system to provide feedback for closed-loop control. The control system cooperates with a load impedance detection circuit, a frequency controllable signal generator and a dynamic impedance matching network to implement closed-loop control of the entire system.

The load impedance detection is realized by a dual directional coupler and the phase amplitude detection chip AD8302. The dual directional coupler is used to sample the incident and reflected waves at the output of the Class E power amplifier. The sampled signal is attenuated and AC coupled to the AD8302 input pin. The AD8302 can convert the amplitude and phase differences of the two input signals into voltage signals. We can detect the voltage value of the AD8302 output pin through the control system to get the amplitude and phase difference between the incident wave and the reflected wave. Thereby calculate the impedance value of several loads. The overall structure of the load detection circuit is shown in Figure 6:

The controller used in the control system is STM32F407. Its high-speed performance and abundant external resources can well meet the design requirements. In this design, the controller mainly completes the closed-loop control of the signal source and the closed-loop control of the dynamic impedance matching network.

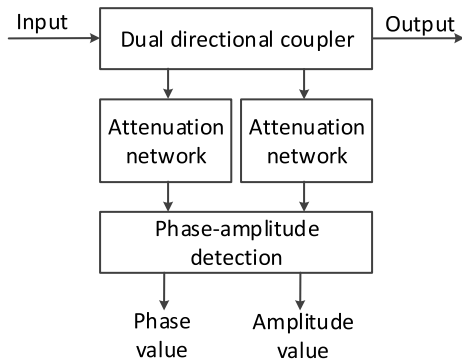


FIGURE 6. Design scheme of load impedance detection device.

**E. THE OVERALL STRUCTURE OF RF POWER**

Figure 7 shows the overall circuit structure of the RF power supply. It can be divided into two parts, the top part is the main component of the RF power supply, and the bottom part is the control part.

In the top part, the MAX038 is used as a signal generator output terminal to be amplified by impedance matching and then connected to a Class E power amplifier. Class E power method devices are followed by a dynamic impedance matching network, a dual directional coupler, and a transmitting coil. The dynamic impedance matching network consists of a fixed inductor and a capacitor array. The capacitor array is controlled by its own relay to determine whether the capacitor is connected to the circuit.

In the bottom part, the output signal of MAX038 is connected to the input capture channel of the controller STM32F407 for frequency sampling after frequency division by 256. It works with the DAC and voltage conversion circuit to achieve closed-loop frequency control. The output signal of the AD8302 is collected by the ADC and calculated by the controller to obtain the load impedance, and then the controller’s 16-channel GPIO control capacitor array is used to implement closed-loop control of dynamic impedance matching.

**III. SYSTEM PARAMETER DESIGN**

In this paper, the maximum DC operating voltage of the RF power supply is 24V, the working frequency band is 11~16MHz (Take ±15% of center frequency), the center frequency (initial working frequency) is 13.56MHz, the center impedance (system initial impedance) is 50 Ω, and the system allows the load lower limit to be 10 Ω. The maximum impedance that can be matched for a dynamic impedance matching network (depending on the operating frequency). According to the above parameters, the following three parts are designed.

**A. PARAMETER DESIGN OF CLASS E POWER AMPLIFIER CIRCUIT**

According to the design requirements, the component parameters of the class E power amplifier are designed and selected. The frequency and load impedance involved in the parameter

calculation process are calculated according to the center value. The main parameters are as follows:

Full load resistance of class E power amplifier:

$$R = \frac{8}{\pi^2 + 4} \frac{V_I^2}{P_O} = 6.64(\Omega) \tag{1}$$

Maximum voltage at both ends of transistor and shunt capacitor:

$$V_{SM} = 3.562V_I = 85.488(V) \tag{2}$$

In Equation (1) and (2), the input voltage is selected as the maximum value of 24V, and the resistance to full load calculated as the output power is selected as 50 W is 6.64 Ω.

According to the above conditions, NXP’s MRF6V2300N is selected as the switching tube of the E-class power amplifier. This is an N-channel enhancement type field effect transistor with a drain-source breakdown voltage of 110V and a maximum output power of 300W [13]. The maximum operating frequency can be up to 600MHz, it can meet the design requirements very well. After selecting the appropriate switch, continue to design the load network parameters:

The resonant inductor  $L_2$  is:

$$L_2 = \frac{Q_L R}{\omega} = 546(nH) \tag{3}$$

The resonant capacitor  $C_2$  is:

$$C = \frac{1}{\omega R \left[ Q_L - \frac{\pi(\pi^2 - 4)}{16} \right]} = 302(pF) \tag{4}$$

It can be calculated that the peak voltages of the resonant inductor and the resonant capacitor can reach 181V and 151V, respectively. Therefore, in consideration of the operating frequency and withstand voltage of the capacitor in the design process, the NPO capacitor with a withstand voltage of 500V is selected as the capacitor of the resonant network, and the inductor is an air-wrapped inductor with an enameled wire. The above are the main parameters and device selection of the class E power amplifier circuit.

**B. DYNAMIC IMPEDANCE MATCHING NETWORK PARAMETER DESIGN**

In class E power amplifiers, under the condition of impedance matching, the output efficiency of the power supply is greatly affected by the Q value of the inductor. Since the Q value of the inductor is difficult to be high in the high frequency circuit, the common high frequency inductance Q value on the market is mostly around 100. The actual part of the impedance actually connected into the circuit cannot be ignored.

Therefore, in order to reduce the influence of the inductance in the load network on the overall efficiency, this paper does not add additional inductance for impedance matching. Instead, the capacitor C2 in the resonance circuit is tapped. The resonant circuit is transformed into the L-shaped impedance matching network transformed in FIG. 5. To achieve the combination of output filtering and

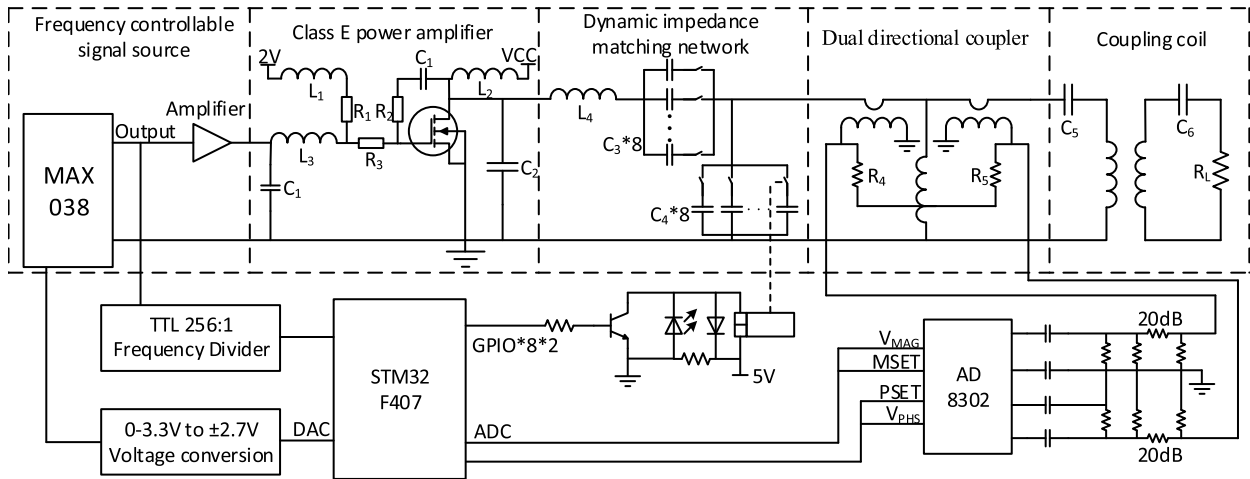


FIGURE 7. A detailed schematic diagram of the entire system.

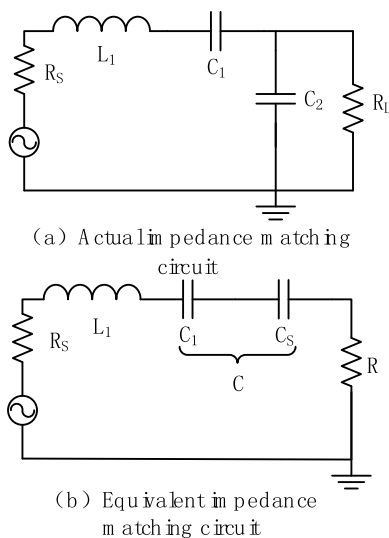


FIGURE 8. Resonant circuit and its equivalent circuit.

impedance matching network. The inductance  $L$  value has been determined during the design of the Class E power amplifier, which is  $546\text{ nH}$ . The following calculations are performed on the capacitors  $C_1$  and  $C_2$  in Figure 8(a).

Through the equivalent circuit in Figure 8(b), we can get the formula for calculating the capacitive reactance of capacitors  $C_1$  and  $C_2$ :

$$X_{C_1} = \frac{1}{\omega C_1} = \left[ Q_L - \frac{\pi(\pi^2 - 4)}{16} - \sqrt{\frac{R_L}{R_S} - 1} \right] R_S \quad (5)$$

$$X_{C_2} = \frac{1}{\omega C_2} = \frac{R_L}{\sqrt{\frac{R_L}{R_S} - 1}} \quad (6)$$

In Equations (5) and (6), the unknowns for calculating the capacitance value are  $\omega$ ,  $R_L$ ,  $R_S$ , and  $Q_L$ , respectively. Among them,  $\omega$  and  $R_S$  are known quantities,  $Q_L$  can be calculated by statistics, and  $R_L$  can be measured by a load detection circuit. Therefore, after the controller obtains  $R_L$  through

measurement and calculation, it can calculate the required capacitance value through the above formula.

After the required capacitance value is calculated, the capacitance value can be changed through the 16-channel GPIO control relay of the controller. Through some preliminary calculations, the resolutions of the capacitors  $C_1$  and  $C_2$  are set to  $10\text{ pF}$  and  $5\text{ pF}$ , respectively. When the high-frequency parasitic effects are ignored, the theoretical change ranges are  $0$  to  $2550\text{ pF}$  and  $0$  to  $1275\text{ pF}$ , respectively. It can achieve dynamic impedance matching in the frequency range of  $11\sim 16\text{ MHz}$  and impedance range of  $10\sim 200\Omega$ .

### C. LOAD IMPEDANCE DETECTION CIRCUIT PARAMETER DESIGN

There are a variety of circuits implemented by dual-directional couplers with centralized parameters. A three-wire transformer is needed in some circuits, and it is difficult to determine the best odd-mode impedance and the best even-mode impedance during the winding process, so it is rarely used in actual production [14], [15]. In this paper, a dual-directional coupler in the form of three transformers is used, which is relatively simple to implement. The actual fabrication circuit is shown in Figure 9.

The main considerations in the design process of the dual directional coupler are working frequency band, insertion loss, coupling degree, isolation, etc. In this paper, the operating band of the dual directional coupler is the operating band of the RF power supply. In addition, since the dual directional coupler actually extracts part of the energy from the system, the insertion loss should be as small as possible to improve the system efficiency.

In the design of dual directional coupler, it is mainly necessary to pay attention to the selection and transformation ratio of the magnetic ring of the transformer (the number of turns on the magnetic ring). Since the dual directional coupler operates at a frequency of  $11\text{--}16\text{ MHz}$ , a nickel-zinc ferrite magnetic ring with good performance in this frequency band is selected [16]. The ratio is closely related to the insertion

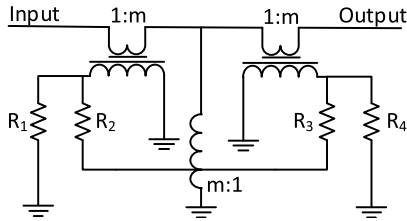


FIGURE 9. Dual directional coupler with three transformer structure.

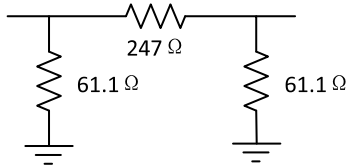


FIGURE 10. 20dB  $\pi$ -type attenuation network.

loss and the degree of coupling. The corresponding mathematical relationship is as follows:

Insertion loss:

$$A_m = 10 \lg \frac{P_O}{P_I} = 10 \lg \frac{4m^6 + 12m^4 + 13m^2 + 6}{4m^6 + 4m^4 + m^2} \quad (7)$$

Coupling:

$$A_C = 10 \lg \frac{P_O}{P_{coup}} = 10 \lg \frac{4m^6 + 4m^4 + 13m^2 + 6}{4m^4 + 8m^4 + 4} \quad (8)$$

In order to reduce the insertion loss as much as possible, we should choose a larger turns ratio, but as the turns ratio increases, the insertion loss decreases more and more slowly, and the number of turns is much more difficult than in the actual production process. Large, so finally choose  $m = 29$  as its turns ratio.

According to Equation 13, the coupling degree is about 29dB. When the system output power is 50W (about 47dBm), the maximum power of the dual directional coupler coupling end can reach 18 dBm. Since the input signal requirement of the AD8302 is less than 0 dBm. It is also necessary to add a 20 dB signal attenuation network between the dual directional coupler and the AD8302. The 20 dB  $\pi$ -type attenuation network is shown in Figure 10.

#### IV. EXPERIMENTAL VERIFICATION

##### A. TESTING OF CLASS E POWER AMPLIFIERS AND DYNAMIC IMPEDANCE MATCHING NETWORKS

The actual parameters of the Class E power amplifier and dynamic impedance matching network are shown in Table 1:

The choke inductor is a high-Q spring-type hollow inductor for radio frequency produced by Coilcraft. Its Q value is typically 114 and the rated operating current is 3A. The resonant inductor is wound using an enameled wire.

The capacitance array is changed according to the actual production as shown in Figure 11:

In Figure 11, the starting value of the parallel capacitance  $C_2$  is large, which is due to the fact that the wiring connected with  $C_2$  is long, the current it passes through is large, and the wiring width is wide, which leads to the relatively large

TABLE 1. Actual parameters of class E power amplifier and dynamic impedance marching network.

Parameter	Value(unit)
maximum operating voltage	24(V)
Frequency Range	11~16(MHz)
choke inductor	246(nH)
bypass capacitor	470(pF)
resonant inductor	540(nH)
parallel capacitance C2	169~1367(pF)
the resolution of C2	4~6(pF)
series capacitor C1	27~2855(pF)
the resolution of C1	9~12(pF)

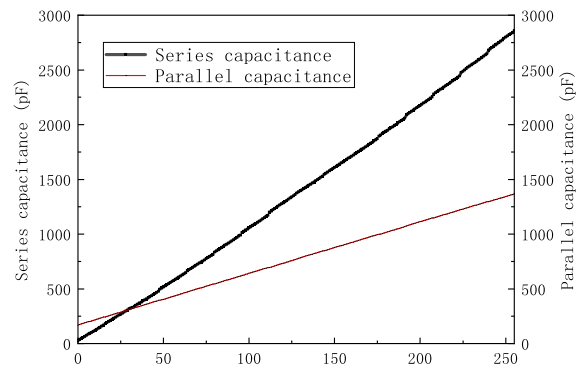


FIGURE 11. Capacitance array measurements, The horizontal axis is the corresponding number ( $1 \sim 2^8$ ) of the capacitor array. The black line represents the capacitance value of the series capacitor  $C_1$ , and the red line represents the capacitance value of the parallel capacitor  $C_2$ .

area between the wiring connected with  $C_2$  and the GND layer, resulting in the large initial value. The linearity of the series capacitor  $C_1$  becomes worse when the capacitance is large, which is because the inductance of the wiring cannot be ignored when the capacitance is large, resulting in the actual capacitance value of the series capacitor becoming larger. In addition, due to the influence of the wiring inductance, the equivalent capacitance of the parallel equivalent capacitance in the dynamic impedance matching network will be reduced compared to a single capacitor. We use the HFSS simulation tool to optimize the PCB design of the dynamic impedance matching network. Make the dynamic impedance matching network have better performance.

##### B. TESTING OF DUAL DIRECTIONAL COUPLERS AND IMPEDANCE MEASUREMENT SECTIONS

Dual directional coupler test results are shown in Table 2:

The output fit curve of the load resistance value and the AD8302 amplitude difference is as shown in Figure 12:

The relationship between the load resistance value and the output voltage value of AD8302 amplitude difference in the figure is not monotonous. When the load is 50  $\Omega$ , there is a maximum value. The output voltage of the same amplitude difference corresponds to two different load resistance values before and after 50  $\Omega$ . This is due to the design impedance of the dual directional coupler being 50  $\Omega$ . For this problem,

TABLE 2. Dual directional coupler test results.

Parameter	VALUE(UNIT)
Insertion loss	0.02~0.03(dB)
Coupling average	29.67(dB)
Isolation minimum	26(dB)
Coupling degree linearity	≤0.06(dB)
VSWR	1.03

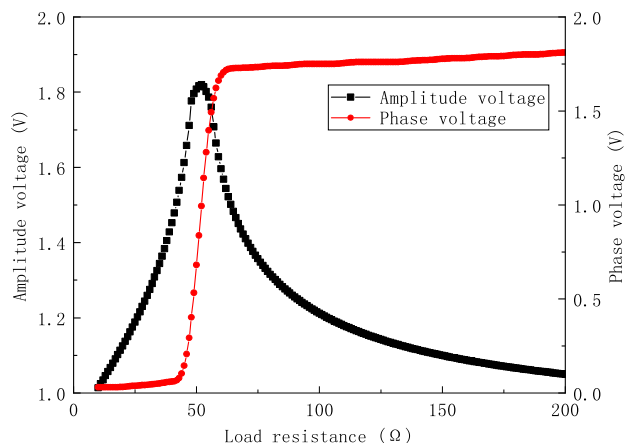


FIGURE 12. Load resistance fit curve, The horizontal axis is the load impedance, the red line represents the voltage value corresponding to the phase difference, and the black line represents the voltage value corresponding to the amplitude difference.

the load resistance value can be distinguished by the phase difference of the output of the AD8302. When the load resistance value is less than 50 Ω, the phase difference should be 180 degrees, so the phase difference output voltage should be about 0V, when the load resistance value is greater than at 50 Ω, the phase difference should be 0 degrees. At this time, the phase difference output voltage should be about 1.8V.

In addition, when the RF power source is used in a wireless power transmission system, the phase difference output voltage of the AD8302 can be used to track the resonant frequency of the transmission coil. When the transmission coil does not undergo frequency splitting, the optimal operating frequency of the system is the coil resonance frequency. At this time, the imaginary part of the system impedance is zero, the incident wave and the reflected wave should be in phase or opposite, and the phase difference output voltage value should be close to 0V or 1.8V. The tracking of the optimal operating frequency of the system after frequency splitting needs further study.

C. PROTOTYPING AND TESTING PLATFORM FOR RF POWER

After completing the various parts of the test, the RF power supply is assembled. The overall RF power supply is shown in Figure 13:

In Figure 13, the first part is class E power amplifier and dynamic impedance matching network, the second part is double directional coupler, the third part is

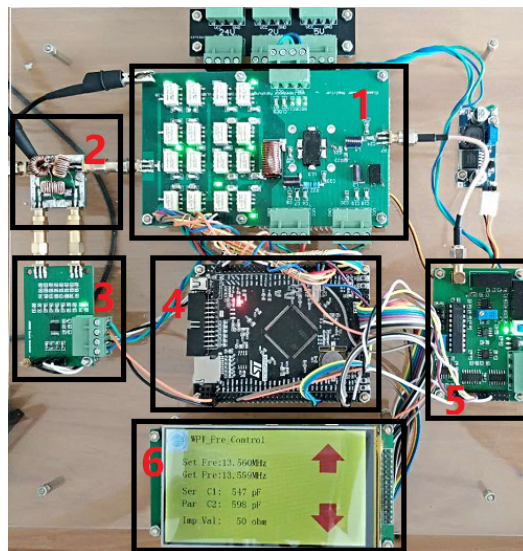


FIGURE 13. The entire composition of RF power supply.

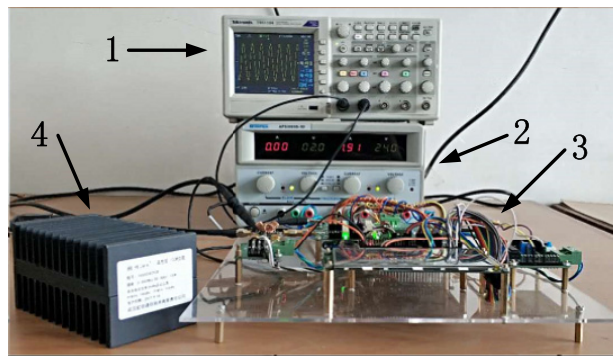
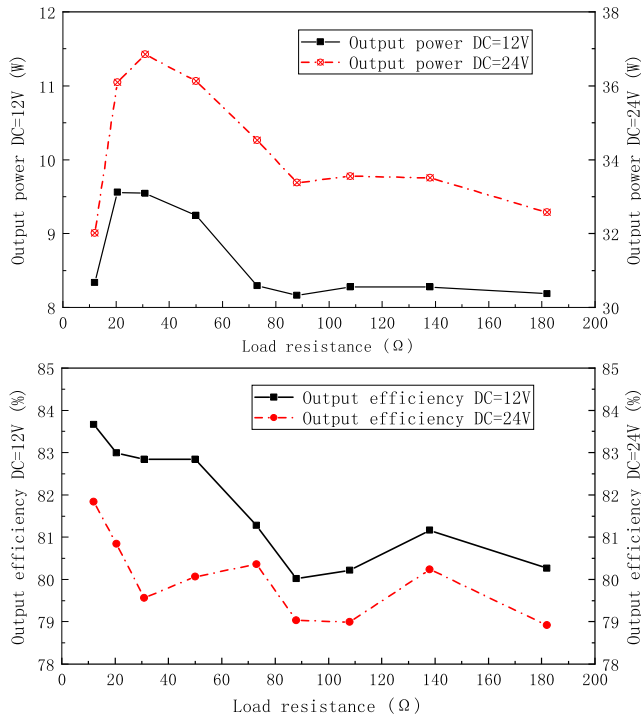


FIGURE 14. RF power supply test platform.

AD8302 phase amplitude detection circuit, the fourth part is STM32F407 control core, the fifth part is MAX038 signal generation circuit, and the sixth part is a LCD human-computer interface supporting touch screen. The parts are connected by coaxial cable or DuPont wire. The LCD and touch screen are added here to display the current working status of the RF power supply and to perform human-computer interaction during the variable frequency test. In actual use, the RF power supply can work without LCD.

After completing the prototype of the RF power supply, we set up a test platform for the RF power output parameters, as shown in Figure 14.

In Figure 14, the first part is an oscilloscope, the second part is an adjustable voltage source, the third part is an experimental test prototype, and the fourth part is a test load. The test load used in this article is a dummy load used in antenna testing. The frequency band used is DC-3GHz, the maximum continuous power is 100W, and the maximum available power in a short time is 300W. Compared with ordinary power loads, it has better high-frequency characteristics, and can basically maintain the same impedance of 50Ω in its frequency and power range.



**FIGURE 15.** Constant frequency variable load test results. The horizontal axis is the load impedance, and the test range is 10~180Ω. The upper picture is the output power, the lower picture is the output efficiency, Black lines and red lines indicate the test results of 12V and 24V working conditions.

**D. RF POWER OUTPUT PARAMETER TEST**

After the platform is built, the output performance of RF power supply is measured. The main test results are constant frequency variable load measurement and constant load variable frequency measurement.

Figure 15 shows the test results of constant frequency variable load. Because the load needs to be replaced in the variable load test, the system impedance is automatically adjusted from the default load to the actual load during each test. After the system is stable, perform measurement and perform 5 measurements, and the interval between each measurement is about 2min. A single test point is the average of 5 measurements. During the test, the working frequency of the system is 13.56MHz.

According to the results in Figure 15, the output power of the RF power supply is relatively stable in the variable load test. The output efficiency is basically stable at over 80% at 12V working voltage, and decreases at 24V working voltage. This is because the resonance inductor is heated seriously due to the large resonance network current at high output power. The measured surface temperature of the resonance inductor is about 40 °C at 12V working voltage. When the working voltage is adjusted to 24V, the surface temperature of the resonance inductor can reach over 70 °C, and the temperature is too high. The resonant inductor here is manually wound using enameled wire. The Q value measured under normal temperature conditions is 78, and the Q value will decrease with increasing temperature under actual working conditions.

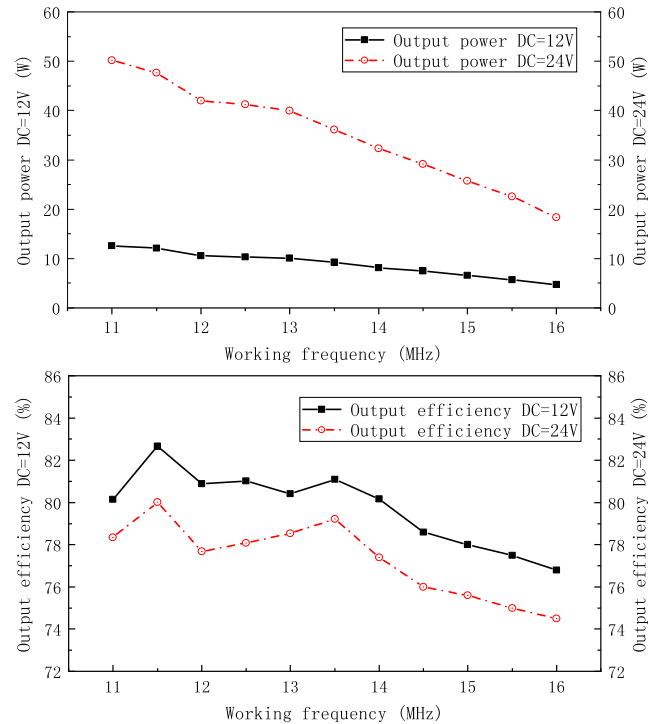


**FIGURE 16.** Constant load variable frequency test results. The horizontal axis is the working frequency, and the test range is 11~16MHz. The upper picture is the output power, the lower picture is the output efficiency, Black lines and red lines indicate the test results of 12V and 24V working conditions.

Based on the above reasons, the operating efficiency of the RF power supply has decreased under the condition that the inductor temperature is too high and the input voltage is high. To solve the above problems, silver-plated copper wires can be used to make high Q inductors. And add a heat sink for the inductor.

Figure 16 shows the test results of constant load and variable frequency. Variable frequency testing can be performed continuously. A test point is selected at 0.5MHz per division from 11 to 16MHz, and each test point is tested after 2 minutes of stable operation. The measurement was performed 5 times in a cycle, and the test results were averaged. During the test, the system load is 50 Ω.

As can be seen from Figure 16, when the frequency changes, the output power will change greatly, and the output efficiency can be stable at more than 75%. However, according to experimental data, higher output power and output efficiency can be obtained at lower operating frequencies. This is because the output power and output efficiency of Class E power amplifiers are affected by the transistor bypass capacitor and choke inductance. And the impact of the bypass capacitor is greater. In the actual design, the bypass capacitor of the transistor is a fixed value. As the operating frequency of the system changes, the bypass capacitor of the Class E power amplifier cannot always be at the optimal value. If the output power of the system is expected to be relatively stable in the entire operating frequency band, a bypass capacitor switching circuit can be added after simulation analysis. The size of



the bypass capacitor can be dynamically adjusted through the dynamic impedance matching network to achieve relatively stable power output in the entire frequency band. The bypass capacitor resolution can be appropriately larger to simplify system design.

The above are the test results of the RF power supply with dynamic impedance matching network. Under the experimental conditions of variable frequency and variable load, the output efficiency can be maintained above 75%. The RF power source previously composed of Class E power amplifiers and fixed impedance matching networks, under the same input voltage and output power conditions. When the operating frequency is 13.56MHz, the lowest efficiency is 55% in the load range of 25Ω~200Ω. When the load resistance is 50Ω, the lowest efficiency is 58% in the frequency range of 12.56MHz~14.75MHz. Relatively speaking, the RF power supply designed in this paper has higher output efficiency over the entire range of variation.

During the entire test process, whether the RF power supply is restarted multiple times during variable load measurement or the RF power supply is continuously operated during variable frequency testing, its output power and output efficiency can be basically maintained steadily. The whole system can work stably during the test.

## V. CONCLUSION

In this paper, the problem of frequency and optimal load of radio energy transmission system is analyzed, and a kind of RF power supply which can adjust the frequency and optimal load resistance of radio energy transmission system is designed. The design scheme of frequency controlled signal source, class E power amplifier circuit, dynamic impedance matching network, load impedance detection circuit and other parts of the power supply are given, and the actual parameters of each part are designed. Finally, the feasibility of the power supply is verified by experiments.

The experimental results show that the power supply can achieve high output efficiency when the frequency and load change in a large range. In view of the problem that the output power changes greatly when the frequency changes, the author gives the corresponding solutions. The experimental scheme is of great significance to solve the problems of frequency and load instability of radio energy transmission system in engineering.

## REFERENCES

- [1] Q. Yang, *Wireless Power Transmission Technology and Its Application*, vol. 8. Beijing, China: China Machine Press, 2014, pp. 1–8.
- [2] M. Budhia, J. T. Boys, G. A. Covic, and C.-Y. Huang, “Development of a single-sided flux magnetic coupler for electric vehicle IPT charging systems,” *IEEE Trans. Ind. Electron.*, vol. 60, no. 1, pp. 318–328, Jan. 2013, doi: [10.1109/TIE.2011.2179274](https://doi.org/10.1109/TIE.2011.2179274).
- [3] H. Hu and S. V. Georgakopoulos, “Wireless power transfer through strongly coupled electric resonance,” in *Proc. IEEE Antennas Propag. Soc. Int. Symp. (APSURSI)*, Orlando, FL, USA, Jul. 2013, pp. 836–837.
- [4] H. Wang and X. Li, “Review and research progress of wireless power transfer for railway transportation,” *IEEJ Trans. Electr. Electron. Eng.*, vol. 14, no. 3, pp. 475–484, Mar. 2019, doi: [10.1002/tee.22829](https://doi.org/10.1002/tee.22829).

- [5] A. M. Jawad, R. Nordin, S. K. Gharghan, H. M. Jawad, and M. Ismail, “Opportunities and challenges for near-field wireless power transfer: A review,” *Energies*, vol. 10, no. 7, p. 1022, Jul. 2017, doi: [10.3390/en10071022](https://doi.org/10.3390/en10071022).
- [6] Q. Zhao, A. Wang, J. Liu, and X. Wang, “The load estimation and power tracking integrated control strategy for dual-sides controlled LCC compensated wireless charging system,” *IEEE Access*, vol. 7, pp. 75749–75761, 2019, doi: [10.1109/ACCESS.2019.2922329](https://doi.org/10.1109/ACCESS.2019.2922329).
- [7] M. Fu, H. Yin, M. Liu, and C. Ma, “Loading and power control for a high-efficiency class E PA-driven megahertz WPT system,” *IEEE Trans. Ind. Electron.*, vol. 63, no. 11, pp. 6867–6876, Nov. 2016, doi: [10.1109/TIE.2016.2582733](https://doi.org/10.1109/TIE.2016.2582733).
- [8] X. Li, X. Dai, Y. Li, Y. Sun, Z. Ye, and Z. Wang, “Coupling coefficient identification for maximum power transfer in WPT system via impedance matching,” in *Proc. IEEE PELS Workshop Emerg. Technol., Wireless Power (WoW)*, Oct. 2016, pp. 27–30, doi: [10.1109/WoW.2016.7772061](https://doi.org/10.1109/WoW.2016.7772061).
- [9] H. Li, J. Li, K. Wang, W. Chen, and X. Yang, “A maximum efficiency point tracking control scheme for wireless power transfer systems using magnetic resonant coupling,” *IEEE Trans. Power Electron.*, vol. 30, no. 7, pp. 3998–4008, Jul. 2015, doi: [10.1109/TPEL.2014.2349534](https://doi.org/10.1109/TPEL.2014.2349534).
- [10] Z. Li, K. Song, J. Jiang, and C. Zhu, “Constant current charging and maximum efficiency tracking control scheme for supercapacitor wireless charging,” *IEEE Trans. Power Electron.*, vol. 33, no. 10, pp. 9088–9100, Oct. 2018, doi: [10.1109/TPEL.2018.2793312](https://doi.org/10.1109/TPEL.2018.2793312).
- [11] M. K. Kazimierczuk, *RF Power Amplifier*, 2nd ed. New York, NY, USA: Tsinghua Univ. Press, 2016, pp. 190–223.
- [12] S. Wang, “The research of RF power supply and impedance matching for wireless power transmission,” M.S. thesis, Elect. Machinery Appl., Dalian Univ. Technol., Dalian, Dalian, 2017.
- [13] L. Hui, L. Ping, and Y. Ya-Meng, “The automatic matching method of RF impedance: Research and design,” *Electron. Opt. Control*, vol. 24, no. 12, pp. 85–94, Dec. 2017, doi: [10.3969/j.issn.1671-637X.2017.12.018](https://doi.org/10.3969/j.issn.1671-637X.2017.12.018).
- [14] Y. Li, Y. Wei, and Q. Wang, “Design method of high efficiency class-E inverter applied to magnetic coupled resonant wireless power transmission system,” *Trans. China Electrotech. Soc.*, vol. 34, no. 2, pp. 219–225, 2019.
- [15] S. Shen, “The design of short wave 3KW concentrated parameter double directional coupler,” *Commun. Countermeasures*, vol. 2001, no. 1, pp. 24–31, 2001.
- [16] J. He, “Design and implementation of lumped parameter directional coupler,” M.S. thesis, Radio Electron., Huazhong Univ. Sci. Technol., Wuhan, China, 2012.



**ZHIHUI HUANG** (Member, IEEE) received the bachelor's and Ph.D. degrees in electrical engineering and electrical appliances from the Dalian University of Technology, in 2006 and 2012, respectively.

Since 2012, he has been a Lecturer with the School of Electrical Engineering, Dalian University of Technology. His research interests include wireless energy transmission, smart appliances, high-voltage appliances, and vacuum switches.



**LEI WANG** (Student Member, IEEE) received the bachelor's degree from the Hebei University of Technology, in 2017. He is currently pursuing the master's degree with the School of Electrical Engineering, Dalian University of Technology.

His main research interests include wireless power transmission and smart appliances.



**YUXING ZHANG** (Student Member, IEEE) received the bachelor's degree from the Changsha University of Science and Technology, in 2016. He is currently pursuing the master's degree with the School of Electrical Engineering, Dalian University of Technology.

His main research interests include wireless power transmission and smart appliances.



**RUITONG LIU** received the bachelor's degree, in 2011. Since 2013, she has been with the State Grid Liaoning Electric Power Research Institute. She is an Engineer. Her main research interest includes power system automation.

...